Fetal Heart-Rate Variability Response to Uterine Contractions During Labour and Delivery

Philip A Warrick[1], Emily F Hamilton[1,2]

[1] PeriGen, Inc, Montreal, Canada
[2] Department of Obstetrics and Gynecology, McGill University, Montreal, Canada

Abstract

Using cardiotocography data from labour and delivery, the objective of this study was to decompose fetal-heart rate variability (fHRV) based on auto-regressive power spectral density analysis into a quiescent component unrelated to contraction and a peak component response to contraction.

During the last 3 hours of labour and delivery, this approach discriminated between normal and pathological fetuses in 15 of 18 epochs for the movement frequency (MF, 150-500 mHz) peak component and 11 of 18 epochs for the low frequency (LF, 30-150 mHz) peak component, and in all epochs of the quiescent components.

These results were superior to previous results based on a longer time window that did not differentiate between contraction and non-contraction intervals. They are also very promising for the improved detection of fetal distress related to hypoxia.

1. Introduction

Labour and delivery is routinely monitored electronically with sensors that measure and record maternal uterine pressure (UP) and fetal heart rate (FHR), a procedure referred to as cardiotocography (CTG). The objective of this monitoring is to detect the fetus at substantial risk of hypoxic injury so that intervention can prevent its occurrence.

In previous work [1, 2], we have studied the deceleration response to contraction, which can be considered the dominating and lowest frequency component response to contraction. In this study, we shift the focus to the contraction response of higher frequency FHR components ($>$ 30mHz), often referred to as fetal heart rate variability (fHRV).

To do so, we constructed short-term (1 min) autoregressive (AR) models at one second increments. An important feature of these models is that we can construct them despite considerable missing data in the analysis interval. Using the AR models, estimates of the power spectral density (PSD) were computed and the spectrum was integrated over low frequency (LF, 30-150 mHz) and movement frequency (MF, 150-500 mHz) bands to obtain two instantaneous components of fHRV. Using overlapping 20 min epochs, the quiescent and peak components of each band were computed from the 5^{th} and 95^{th}percentiles of their probability distribution functions. We compared these short-time window fHRV estimates to those that we have used in previous studies based on a autocorrelation window equal to the 20 minute epoch length.

This work is related to that of a study on a small sample of healthy fetuses, which found that there were FHR responses to contractions at frequencies quite different from the contractions themselves, and with frequency-dependent lags [3]. Our study draws from a much larger and varied population of fetuses in order to attempt to draw conclusions about the discriminatory power of this approach.

2. Methods

2.1. Data

The data consisted of 360 cardiotography (CTG) recordings of singleton, term pregnancies having no known congenital malformations, with at least three hours of tracing just prior to delivery. Each tracing was labelled by outcome information available after delivery (blood gases and neurological assessment). 68 of the cases were normal (N) and 292 were severely pathological (P).

Data collection was performed by clinicians using standard clinical fetal monitors to acquire the CTG. The monitors reported at uniform sampling rates of 4 Hz for FHR (measured in beats per minute (bpm)) and 1 Hz for UP (measured in mmHg), which we up-sampled to 4 Hz by zero-insertion and low-pass filtering. In the majority of cases, the UP or FHR sensors were attached to the maternal abdomen; the FHR was acquired from an ultrasound probe and the UP was acquired by tocography. In a few cases, they were acquired internally via an intra-uterine

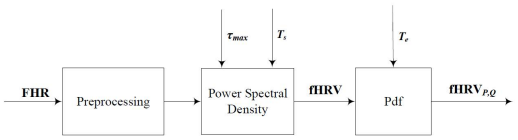

Figure 1. Block diagram of overall processing

(IU) probe and/or a fetal-scalp electrode.

2.2. Overall approach

As shown in Fig. 1 the acquired FHR signal was preprocessed to interpolate missing data and extract the fHRV components (> 30 mHz). Using short-term ($\tau_{\mathbf{max}}$=1 min) autoregressive models constructed at $\mathbf{T_s}$=1 s increments, power spectral density (PSD) estimates were computed and the spectrum was integrated over low frequency (LF, 30-150 mHz) and movement frequency (MF, 150-500 mHz) bands to obtain two instantaneous components of **fHRV**. Using overlapping $\mathbf{T_e}$=20 min epochs, the quiescent and peak components $\mathbf{fHRV_{P,Q}}$ of each band were computed from the 5^{th} and 95^{th}percentiles of their probability distribution functions.

2.3. Preprocessing

The CTG data was recorded in a clinical setting, so it was subject to specific types of noise. The loss of sensor contact can temporarily interrupt the UP or FHR signals, and interference from the (much lower) maternal heart rate can corrupt the FHR. These both appeared in the signal as a sharp drop to much lower amplitude followed by a sharp signal restoration. We preprocessed the data to bridge these interruptions with linear interpolation.

The FHR was then detrended by a high-pass filter with cutoff frequency 30 mHz, corresponding to the lower limit of the LF band of fetal HRV [4].

2.4. Power spectral density (PSD)

We computed a power spectral density using a autoregressive model using an approach similar to that taken in [2], except that all bridged intervals were excluded from consideration in the autocorrelation estimation to reduce bias introduced by the linear interpolation. The amount of missing data was monitored to provide subsequent assessment of the confidence in the PSD estimates.

2.4.1. Autocorrelation

We modified the calculation of the conventional FHR autocorrelation estimate r_f to exclude the intervals where the signal had been interpolated in the preprocessing step. Therefore, the revised estimate for a window of n samples was:

$$r_f(k) = \frac{1}{n_k} \sum_{i=0}^{n-1} \sum_{k=0}^{N-1} f(i) f(i-k) \tag{1}$$

where N is the longest lag and each term $f(i)f(i-k)$ is included in the sum if and only if both $f(i)$ and $f(i-k)$ are non-interpolated samples and n_k is the total number of $f(i)f(i-k)$ terms included at lag k.

2.4.2. Autoregressive (AR) model

Similar to the method described in [2], we used the autocorrelation estimates to compute coefficients of an AR model using linear prediction via the Levinson-Durbin algorithm and chose the model order p using the minimum-description length (MDL) criterion. Power spectral densities (PSD) of the AR models were computed following [6] and sampled at 128 frequencies between 0 and the Nyquist frequency of 2 Hz to resolve the majority of the resonances.

2.5. Quiescent and peak fHRV

We estimated successive PSDs of the fHRV at intervals of $\mathbf{T_s}$=1 s using a maximum lag $\tau_{\mathbf{max}}$=1 min of the autocorrelation function r_f. At each time interval j, the LF and MF PSD bands were summed to give instantaneous bands estimates $fHRV_{LF}(j)$ and $fHRV_{MF}(j)$. The square-root magnitude of these band sums were computed to transform them to bpm units for more convenient comparison with the acquired FHR.

The probability distribution function (pdf) of the instantaneous band signals was then computed over an epoch of $\mathbf{T_e}$=20 min. The quiescent and peak components $\mathbf{fHRV_{P,Q}}$ of each band were computed from the 5^{th} and 95^{th}percentiles of their pdfs. The epoch was advanced at 10 minute intervals over the course of the labour and delivery.

We compared these short-time window fHRV estimates to those that we have used in previous studies [2] based on a maximum lag of the autocorrelation window equal to the 20 min epoch length.

3. Results

Fig. 2 shows the acquired UP and FHR signals as well as the quiescent and peak signals over a typical epoch. It is clear that the fHRV components are relatively flat between the peaks of the UP (i.e. the uterine contractions), while the components generally peak in response to the uterine contraction. The LF components tend to dominate the MF components, but their time courses are similar.

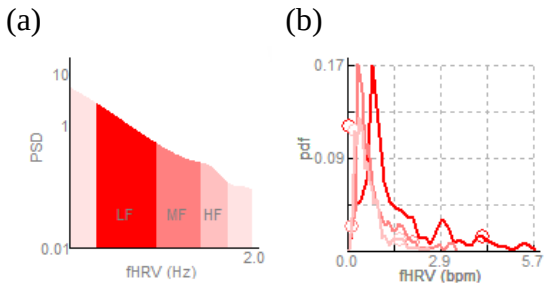

Figure 3. from a typical epoch, (a) power spectral density (PSD) estimates with the LF and MF bands indicated and (b) Probability distribution functions (pdfs) of the $\mathbf{fHRV_{P,Q}}$ components for each of the LF (red) and MF (dark pink) bands. The circles indicate the 5^{th} and 95^{th} percentiles of each distribution. A high frequency (HF) band is also shown (light pink), but not included in this analysis.

Note that we have not shown the high-pass version of the fHRV which should exclude most of the energy in the deceleration band (which is below the lower LF band limit of 30 mHz). Therefore the information in these fHRV peaks are complementary to the deceleration response to contraction visible in Fig. 2 and more thoroughly studied in [2].

Fig. 3 shows a PSD and associated pdfs of the fHRV components that describe the range of the LF and MF components in terms of their 5^{th} and 95^{th}percentiles for the typical epoch described above.

We then examined the time course of the quiescent and peak fHRV between between N and P classes over the course of the last three hours of labour and delivery. Fig. 4 shows that compared to the N cases, the P cases had peak components for both bands that were consistently higher and quiescent components that were consistently lower in magnitude. Specifically, the MF_p component had statistically significant class differences in 15/18 epochs (compared to 11/18 epochs for the MF_m) and was contiguous from -180 to -40 min, including later epochs -80 to -30 min where the MF_m differences were not significant. The LF differences were equal in number (11) for the LF_m and LF_p components. The quiescent components were consistently discriminating for both bands.

Average continuity (not shown) early in the three hour period was lower for of the P cases compared to the N cases (85% and 95%, respectively) while both dropped by the end of labour (to 77% and 85%, respectively). This likely reflects the increasing movement of the mother late in labour as well as the greater degree of intervention for fetuses with non-reassuring CTG.

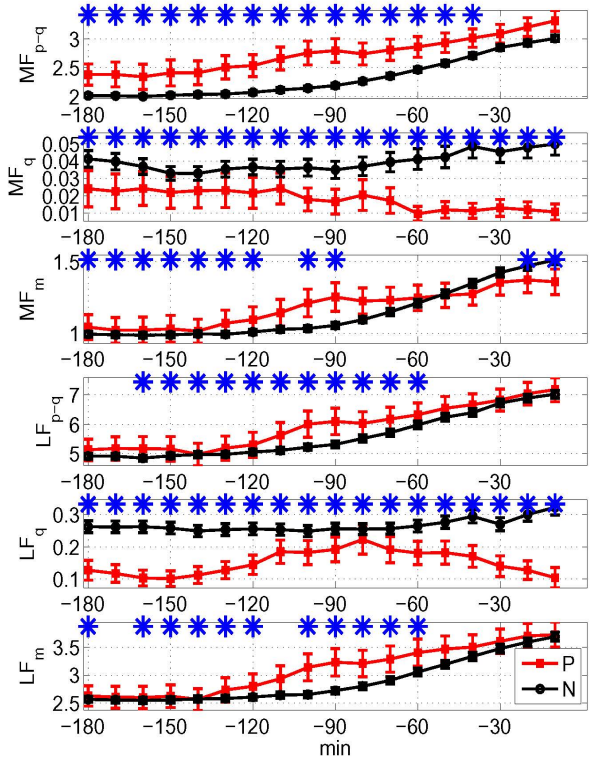

Figure 4. Fetal HRV estimates during the last 3 hours of labour and delivery for normal (n_N=292) and pathological (n_P=68) cases: The m, q and p subscripts of the LF and MF bands refer to mean, quiescent and peak levels, respectively. The units on the vertical axis are beats per minute. The means are plotted with bars indicating standard error and the blue asterisks indicating statistically significant differences between normal and pathological cases at that epoch (p <0.05, Kolmogorov-Smirnov distribution test).

4. Conclusions

Overall for both LF and MF bands, the p-q components resemble the m components, except that there is more separation between the two classes in the p-q estimates. This suggests that the separation of the fHRV into these two components provides more information than the mean estimate, whose shape is dominated by the peak values.

In subsequent work we will investigate the timing of the fHRV response with respect to the uterine contractions, including the smoothing effects of the 1 minute autocorrelation window. We are also applying this analysis to a population of cases than experienced metabolic acidosis but without neurological injuries. Our preliminary results indicates that the peak components of this intermediate population tends to greater magnitudes similar to the pathological

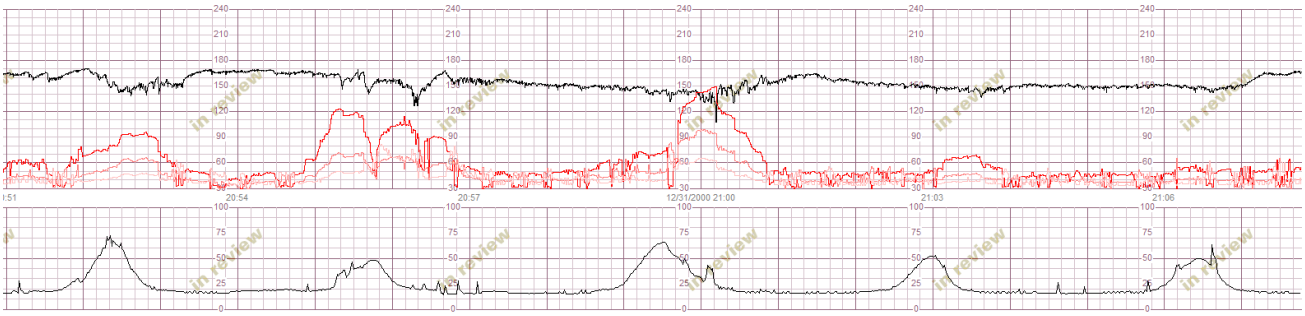

Figure 2. Acquired FHR and UP signals (in black, top and bottom respectively) as well as the computed $\mathbf{fHRV_{P,Q}}$ components (LF and MF bands are in darker and lighter red, respectively). The acquired signals are to scale with the units as shown (30 to 240 bpm), but the fHRV signals have been magnified for clarity (their vertical scales have limits of 0 and 10 bpm).

cases. Timely indentification of such 'close calls' would be helpful for the intervention and prevention of hypoxia-related sequelae.

References

[1] Warrick PA, Hamilton EF, Precup D, Kearney RE. Identification of the dynamic relationship between intra-partum uterine pressure and fetal heart rate for normal and hypoxic fetuses. IEEE Transactions on Biomedical Engineering 2009; 56(6):1587–1597.

[2] Warrick P, Hamilton E, Precup D, Kearney R. Classification of normal and hypoxic fetuses from systems modeling of intrapartum cardiotocography. IEEE Transactions on Biomedical Engineering 2010;57(4):771–779. ISSN 0018-9294.

[3] Romano M, Bifulco P, Cesarelli M, Sansone M, Bracale M. Foetal heart rate power spectrum response to uterine contraction. Medical and Biological Engineering and Computing 2006;44:88–201.

[4] Signorini M, Magenes G, Cerutti S, Arduini D. Linear and nonlinear parameters for the analysis of fetal heart rate signal from cardiotocographic recordings. IEEE Transactions on Biomedical Engineering 2003;50(3):365–374. ISSN 0018-9294.

[5] Westwick DT, Kearney RE. Identification of nonlinear physiological systems. Hoboken NJ: Wiley-Interscience, 2003.

[6] Cerutti S, Civardi S, Bianchi A, Signorini M, Ferrazzi E, Pardi G. Spectral analysis of antepartum heart rate variability. Clin Phys Physiol Meas 1989;10:27–31.

Address for correspondence:

Philip A. Warrick

PeriGen Inc. (Canada) 5252 deMaisonneuve boul., suite 314, Montreal, Quebec H4A3S5 Canada

philip.warrick@perigen.com